

## Supplemental Material

**Table S.1.** Comparison of the energy data for mineral phases and a  $S^{6+}$  incorporation reaction involving those phases that are calculated using the PBE and PW91 functional.

Mineral phase	Calculated Energy (eV)		Energy difference (eV) (A-B)
	PBE (A)	PW91 (B)	
$Ca_{10}(PO_4)_6F_2$	-22974.86	-22996.08	21.22
$Ca_{10}(PO_4)_6Cl_2$	-22465.91	-22486.54	20.63
$Ca_{10}(PO_4)_6(OH)_2$	-22553.65	-22574.60	20.96
$Ca_9Na(PO_4)_5(SO_4)F_2$	-23368.63	-23390.21	21.58
$Ca_9Na(PO_4)_5(SO_4)Cl_2$	-22859.89	-22880.89	21.00
$Ca_9Na(PO_4)_5(SO_4)(OH)_2$	-22947.49	-22968.81	21.32
$CaSO_4$	-3031.46	-3034.33	2.86
$Ca_3(PO_4)_2$	-6879.65	-6886.06	6.41
$Na_3(PO_4)$	-5848.99	-5854.26	5.27
Incorporation reaction	$\Delta E_{rxn}$ (eV)		Energy difference (eV) (A'-B')
$Ca_{10}(PO_4)_6X_2 + 1/3Na_3PO_4 + CaSO_4 \leftrightarrow [Ca_9Na][(PO_4)_5(SO_4)]X_2 + 2/3Ca_3(PO_4)_2$	PBE (A')	PW91(B')	
X = F	0.93	0.91	0.01
Cl	0.85	0.83	0.01
OH	0.72	0.69	0.03

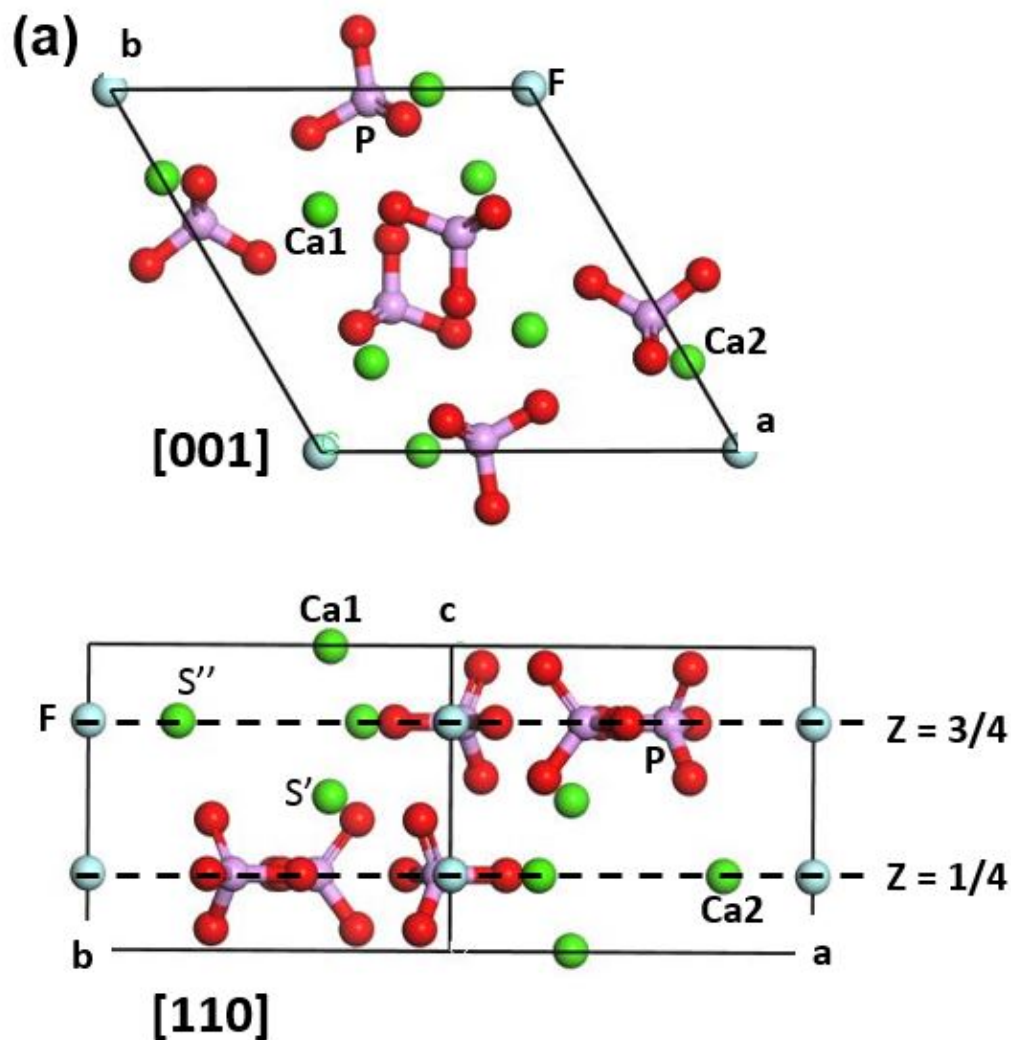


Figure S.1 (a)

**Figure S.1.** Different views for the bulk structure of the apatite end members used in this study. (a) fluorapatite  $[Ca_{10}(PO_4)_6F_2]$  (b) chlorapatite  $[Ca_{10}(PO_4)_6Cl_2]$  and (c) hydroxylapatite  $[Ca_{10}(PO_4)_6(OH)_2]$ . In (a) and (b), the positions of  $Cl^-$  and  $OH^-$  below the planes at  $z = 1/4$  and  $3/4$  were selected such that symmetry reduction from  $P6_3/m$  to the  $P6_3$  group occurs for chlora- and hydroxylapatite.  $S'$  and  $S''$  in (a) and (b) denotes the  $Ca1$  and  $Ca2$  site replaced by  $Na^+$  to test the effect of site preference of sodium on  $S^{6+}$  incorporation into apatite.

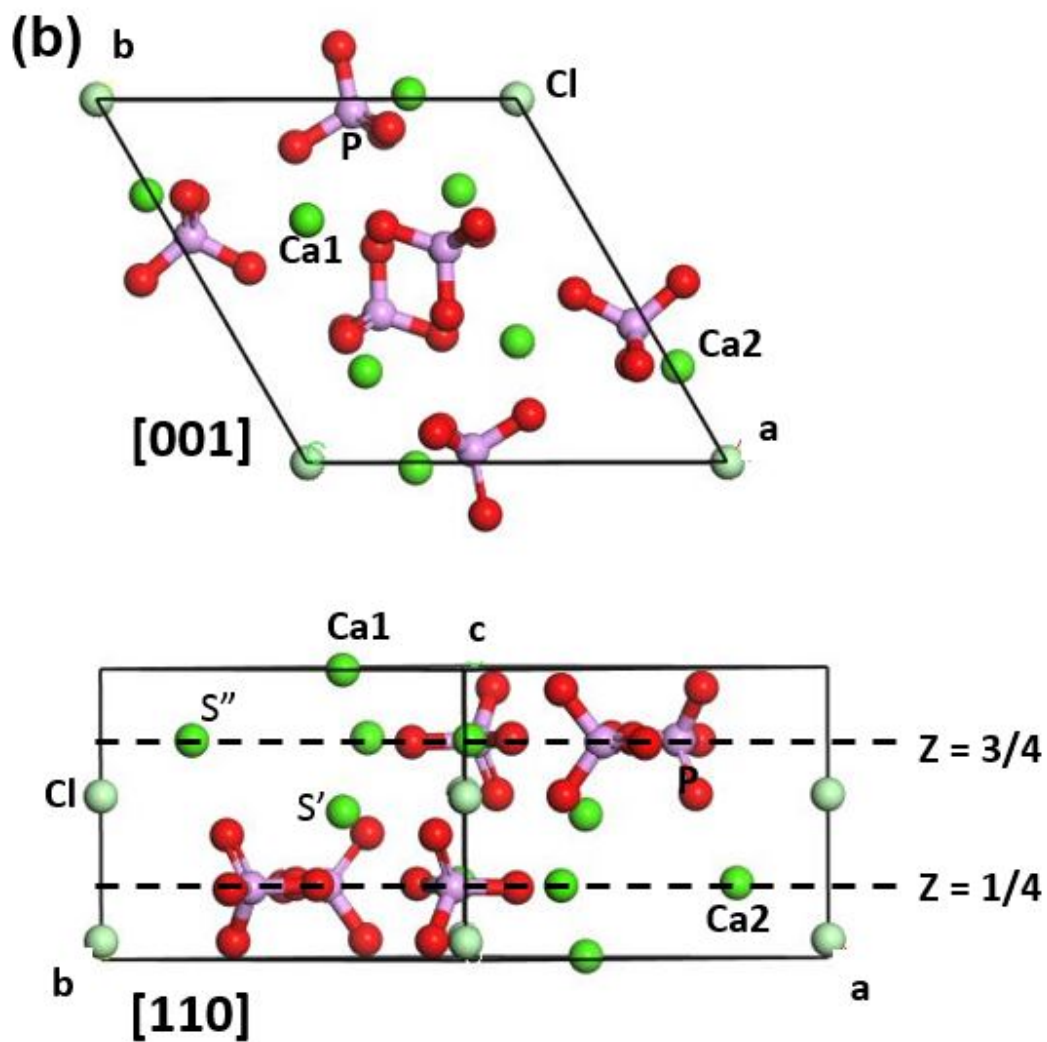


Figure S.1 (b)

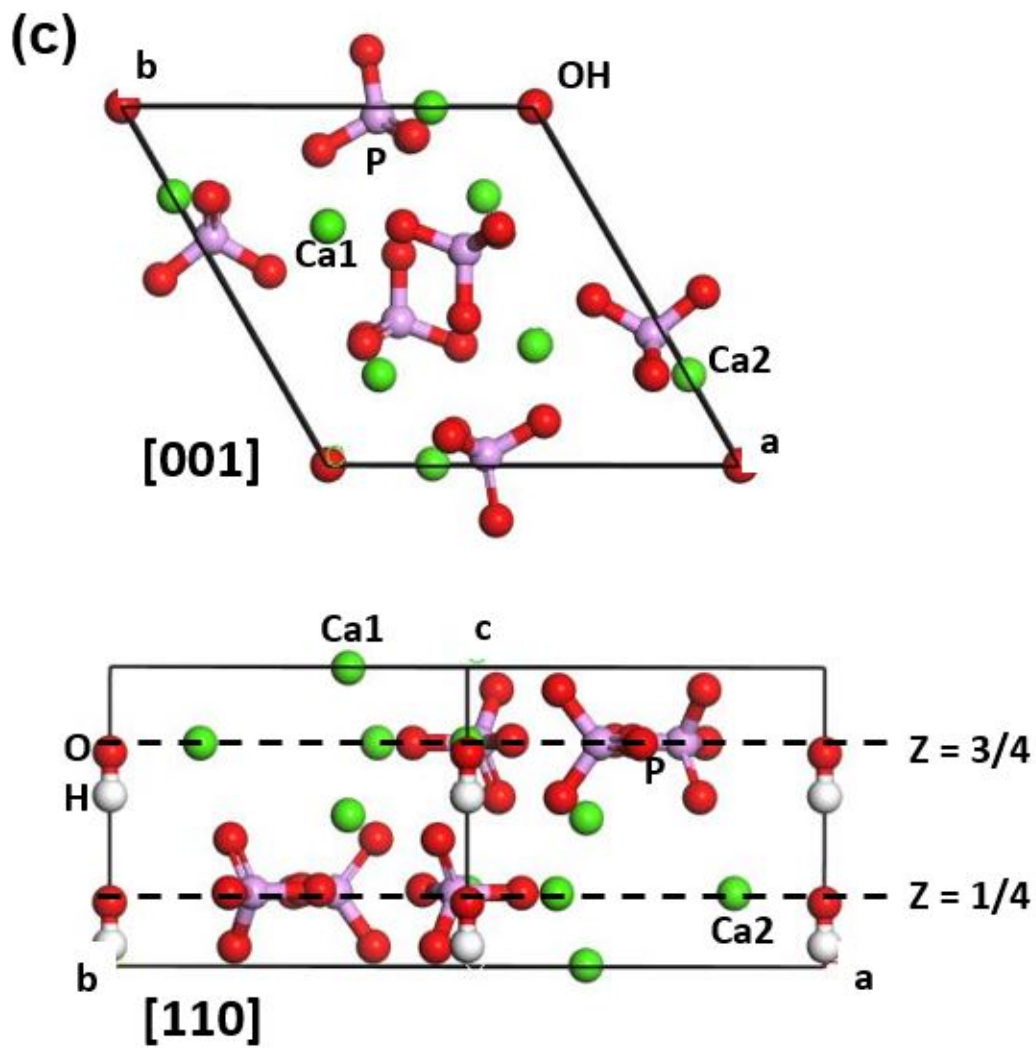


Figure S.1 (c)

## Electronic structure of S incorporated apatite

Energy-dependent density of states (DOS) analysis is used to obtain electronic structure of the S incorporated apatite configurations investigated in this study. The density of states (DOS) can be further resolved into partial density of state (PDOS) plots for certain angular momenta on atoms of interest (s, p, and d orbital characters in this study). The PDOS spectrum for fluorapatite without incorporated S atom is shown in Figure S.2. Each peak is labeled to represent orbital contributions of atoms for the peak. The major contributions to the apatite PDOS are the 3s and 3p orbitals of phosphorous (P) and the 2s and 2p orbitals of oxygen (O), the latter one forming  $\sigma$  bonds to P 3p orbitals. The O 2p orbital character of the  $\text{PO}_4^{3-}$  group is within the range of -10 to 0 eV and is the main contributions to the four p bands labeled A to D in Figure S.2. Peak A and D are primarily composed of O 2p states, whereas the contributions of P 3p and F 2p are included in peak B and C, respectively. The main contributions of Cl 3p states are also at peak C in the chlorapatite PDOS (not shown). These four peaks (A to D) are consistent with a previous report on the electronic structure of calcium phosphate crystals (Rulis et al. 2004).

Even upon the S oxyanion incorporation, the apatite PDOS is contributed mainly from the states of the phosphate group because only one or two of six phosphates are replaced by  $\text{SO}_4^{2-}$  or  $\text{SO}_3^{2-}$  in this study (Fig. S.2). For this reason, the four major p orbital peaks are labeled A to D for PDOS spectra of both apatite and the  $\text{PO}_4^{3-}$  group in Figure S.3. The 2p character of the  $\text{SO}_4^{2-}$  and  $\text{SO}_3^{2-}$  groups reveals four main peaks at -10 to 0 eV, labeled A\* to D\*. In  $\text{S}^{6+}$  incorporated apatite,  $\text{Ca}_{10}(\text{PO}_4)_4(\text{SiO}_4)(\text{SO}_4)\text{F}_2$ , the positions of peak A\* to D\* (the  $\text{SO}_4^{2-}$  group) are 1.0 to 2.5 eV lower than peak A to D ( $\text{PO}_4^{3-}$ ). In the PDOS spectra of the  $\text{S}^{6+}$ -incorporated apatite, the highest peak C\* of sulfate is located at an energy region between B and C (Fig. S.2a). In  $\text{S}^{6+}$  and  $\text{S}^{4+}$  co-incorporated fluorapatite with A-type sulfite,  $\text{Ca}_9\text{Na}(\text{PO}_4)_3(\text{SiO}_4)(\text{SO}_4)(\text{SO}_3)\text{F}_2$ , the energy difference in the

peaks between the  $\text{SO}_4^{2-}$  and  $\text{PO}_4^{3-}$  groups are 0.8 to 2.3 eV while the positions of peak A\* to D\* in the  $\text{SO}_3^{2-}$  group are 0.8 to 1.1 eV higher than those in the  $\text{SO}_4^{2-}$  group (Fig. S.2b). It is worthy to note that peak C\* and D\* appear as doublet for the  $\text{SO}_3^{2-}$  group. The doublet of C\* and D\* is positioned at -3.2/-1.8 eV and -1.1/-0.20 eV, respectively. The p orbital contribution to one at -0.2 eV is composed primarily of the non-bonding S 3p states of S (i.e., the lone pair electrons) and account for some of the states just below the Fermi level ( $E_{\text{Fermi}} = 0$  eV).

The PDOS spectrum of  $\text{S}^{2-}$  incorporated fluorapatite is shown in Figure S.4 as an example of partial  $\text{S}^{2-}$  incorporation on a  $\text{Cl}^-$  position. The sulfide ( $\text{S}^{2-}$ ) ion at the column site reveals the S 3p and 3s states peaks at -0.1 and -9.5 eV, respectively. The S 3p states mainly contribute to an energy region just below the Fermi level ( $E_{\text{Fermi}} = 0$  eV). The PDOS of  $\text{S}^{2-}$  is compared with the other S oxidation states,  $\text{S}^{4+}$  and  $\text{S}^{6+}$  ions in apatite with A-type sulfite (Fig. S.3b to d). Although the non-bonding 3p states of  $\text{S}^{4+}$  are close to the energy level of the  $\text{S}^{2-}$  3p states, the other occupied 3p orbital states are shifted to lower energy levels forming bonds with surrounding O in the sulfite molecule. The occupied S 3p states are shifted to more negative energy levels in the sulfate molecule indicating an energy lowering by bonding between S and O. Such difference in the PDOS spectra between sulfide and sulfur oxyanions may reflect the ionic character of sulfide interacting with surrounding Ca ions in the apatite structure (Rulis et al. 2004).

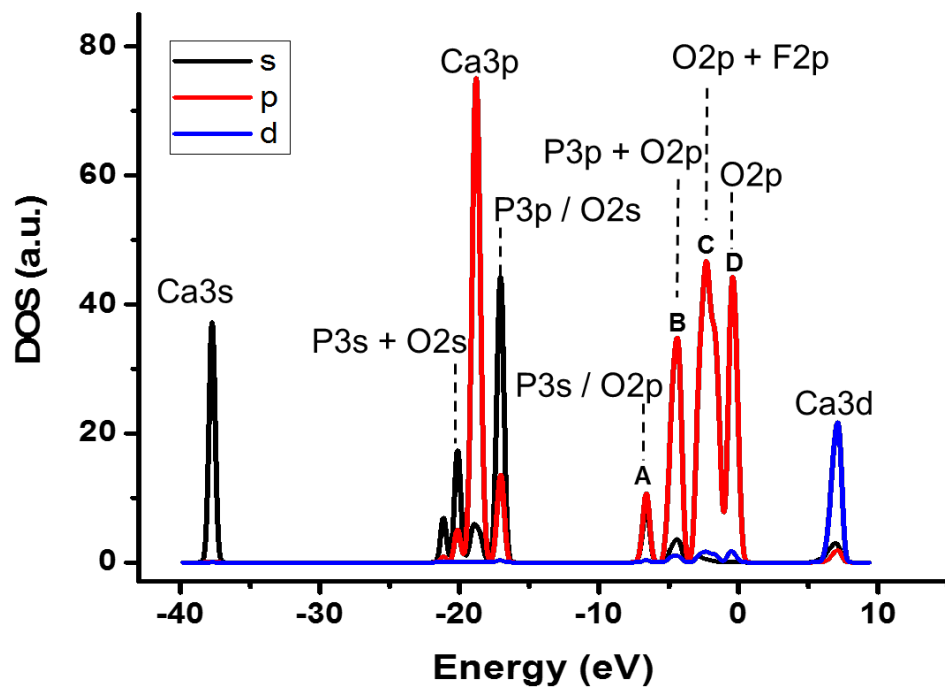


**Figure S.2.** Calculated density of states (DOS) spectra for fluorapatite without sulfur incorporation.

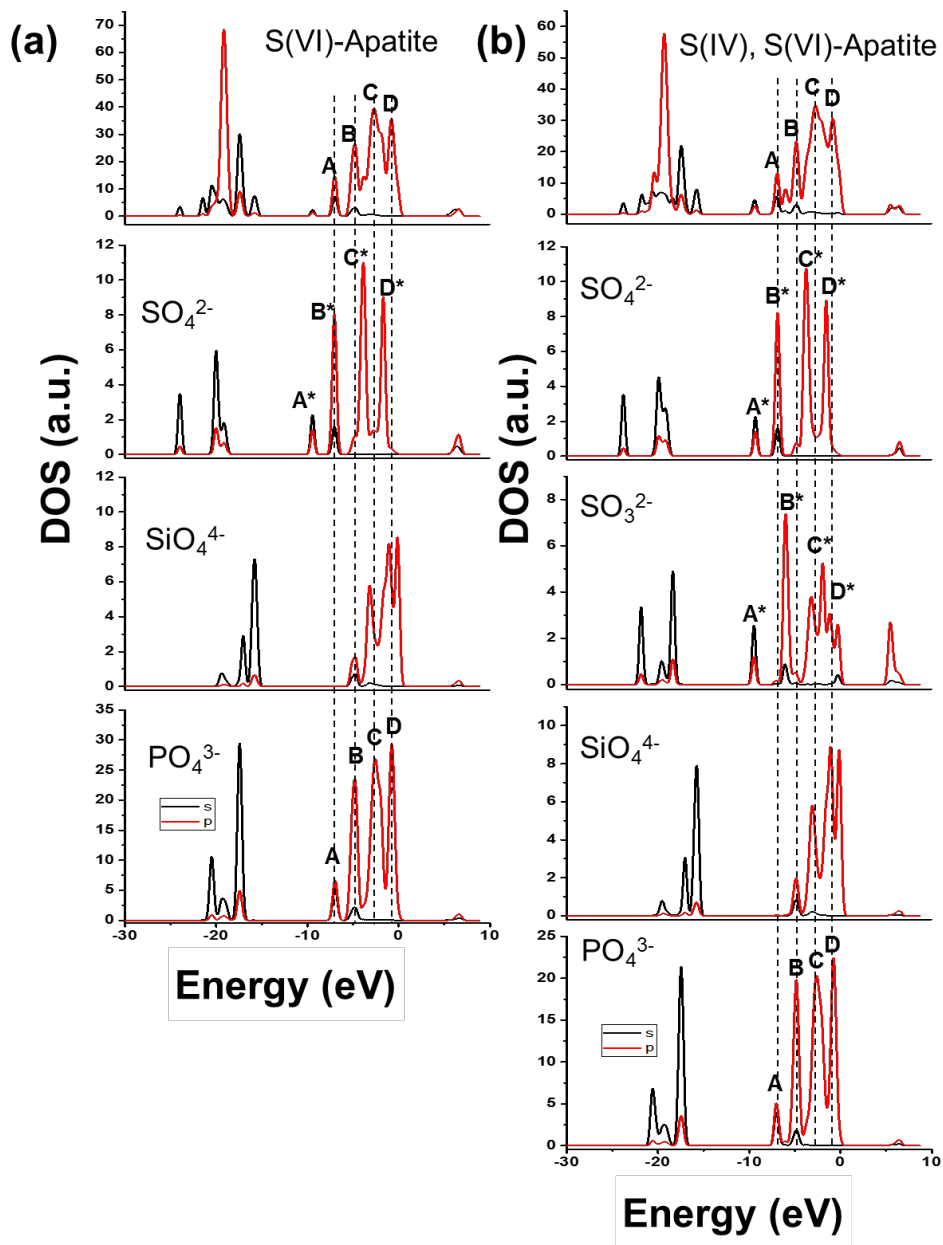


**Figure S.3.** PDOS spectra of (a)  $S^{6+}$  incorporated fluorapatite,  $Ca_{10}(PO_4)_4(SiO_4)(SO_4)F_2$ , and of (b)  $S^{6+}$  and  $S^{4+}$  co-incorporated fluorapatite,  $Ca_9Na(PO_4)_3(SiO_4)(SO_4)(SO_3)F_2$ . Top: PDOS spectrum of each apatite phase; PDOS spectra of the anion groups consisting of the apatite phases are shown sequentially. The four major p orbital state peaks at -10 to 0 eV are labelled A to D in PDOS spectra of apatite and the  $PO_4^{3-}$  group, and A\* to D\* in that of the  $SO_4^{2-}$  and  $SO_3^{2-}$  group.

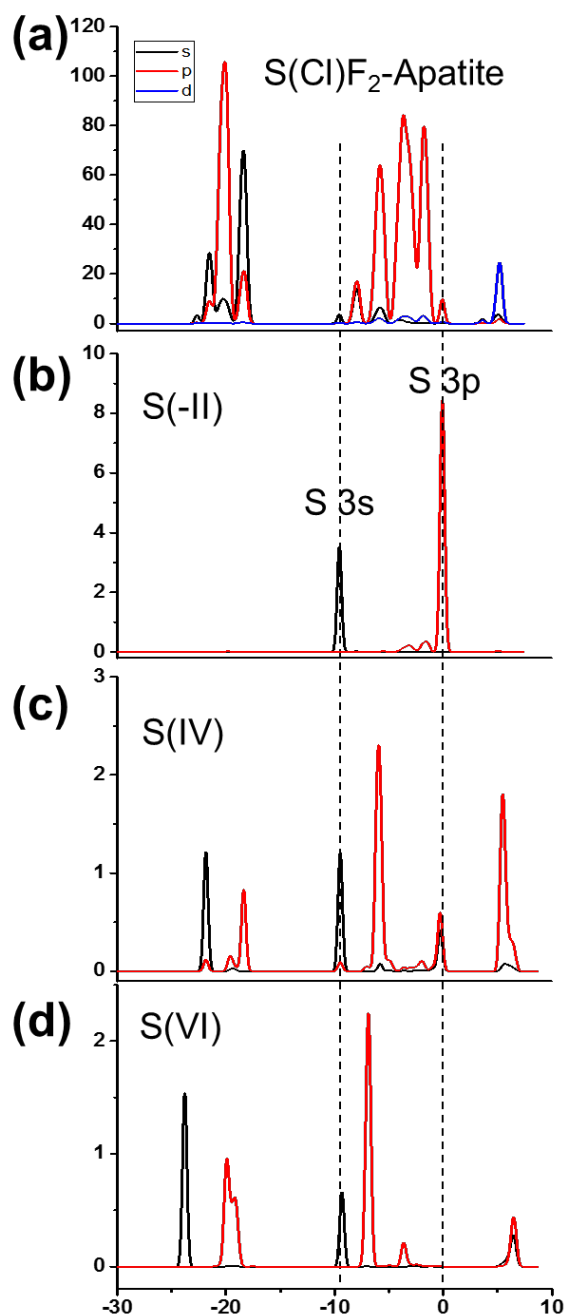


**Figure S.4.** PDOS spectra of (a) S<sup>2-</sup> incorporated fluorapatite, Ca<sub>20</sub>(PO<sub>4</sub>)<sub>12</sub>SF<sub>2</sub> and (b) S<sup>2-</sup> in the structure. PDOS of (c) the S<sup>4+</sup> and (d) S<sup>6+</sup> ions in S<sup>6+</sup> and S<sup>4+</sup> co-incorporated fluorapatite with A-type sulfite, Ca<sub>9</sub>Na(PO<sub>4</sub>)<sub>3</sub>(SiO<sub>4</sub>)(SO<sub>4</sub>)(SO<sub>3</sub>)F<sub>2</sub>, are also presented for comparison.